Supplementary Material: Field-induced Metal-Insulator Transition in β-EuP_3

Guangqiang Wang,[1] Guoqing Chang,[2] Huibin Zhou,[1] Wenlong Ma,[1]
Hsin Lin,[3] M. Zahid Hasan,[2,4] Su-Yang Xu,[5] and Shuang Jia[1,6,7,8,*]

[1] *International Center for Quantum Materials, School of Physics, Peking University, Beijing 100871, China*
[2] *Laboratory of Topological Quantum Matter and Advanced Spectroscopy (B7), Department of Physics, Princeton University, Princeton, NJ, USA*
[3] *Institute of Physics, Academia Sinica, Taipei 11529, China*
[4] *Lawrence Berkeley National Laboratory, Berkeley, CA, USA*
[5] *Department of Physics, Massachusetts Institute of Technology, Cambridge, Massachusetts 02139, USA*
[6] *Collaborative Innovation Center of Quantum Matter, Beijing 100871, China*
[7] *CAS Center for Excellence in Topological Quantum Computation, University of Chinese Academy of Sciences, Beijing 100190, China*
[8] *Beijing Academy of Quantum Information Sciences, Beijing 100193, China*

(Dated: August 25, 2020)

Identification of the β-EuP_3 phase by using powder X-ray diffraction

The low-temperature phase of β-EuP_3 was grown by cooling down the melted mixed raw materials. In order to confirm the resultant crystals, Cu-K_α powder X-ray diffraction (XRD) measurement was conducted at room temperature in a Rigaku MiniFlex-600 diffractometer. Figure S1 shows the XRD pattern for β-EuP_3 in which the peaks obtained through Rietveld refinement are labeled. The XRD pattern matches well with the one in earlier experiment [1].

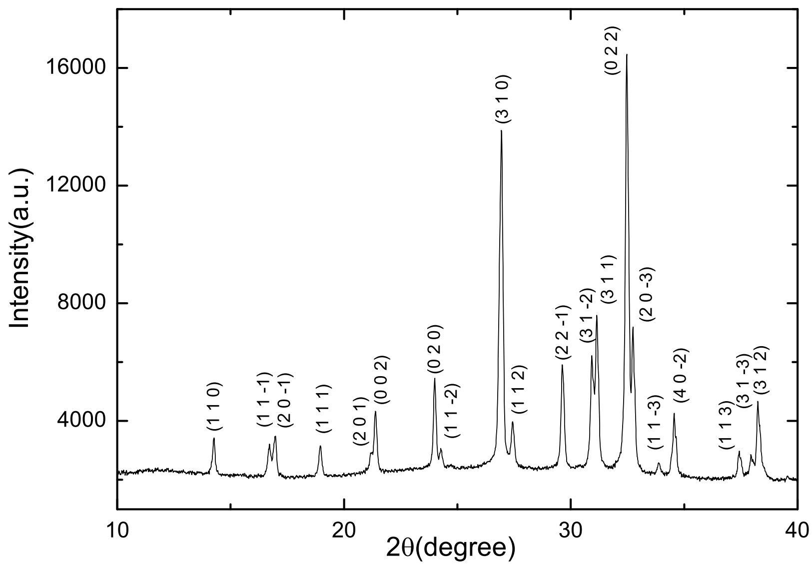

Fig. S1. The powder XRD pattern for β-EuP_3 in which the peaks are indexed with (hkl).

Isothermal $M(H)$ curves for β-EuP_3

Figure S2 shows the $M(H)$ curves at different temperatures for β-EuP_3. The saturated magnetization is above 7.2 μ_B/formula unit (f.u.) at 2 K, very close to the value for the $4f^7$ spin configuration of the $^8S_{7/2}$ Hund's ground state of Eu^{2+} cation.

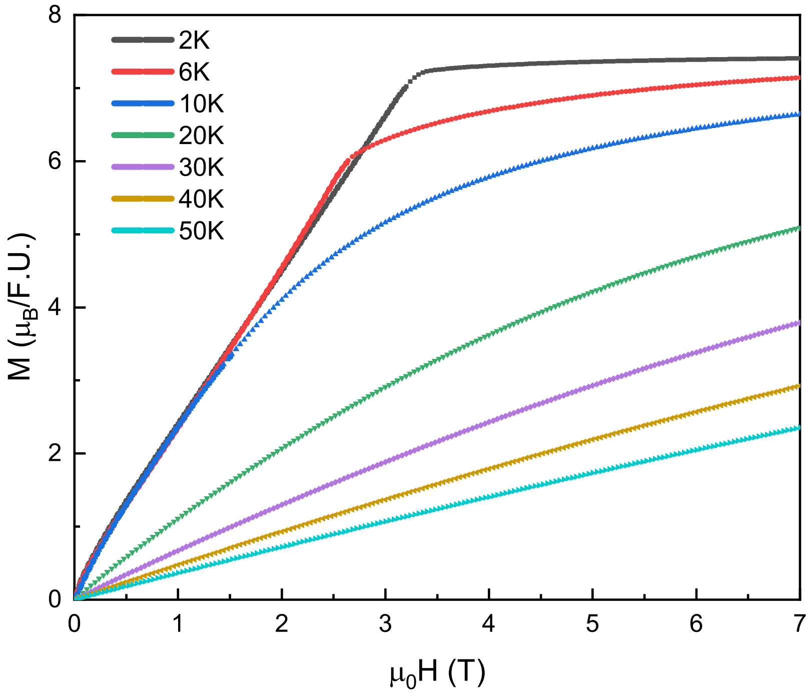

Fig. S2. $M(H)$ for β-EuP_3 at different temperatures when the field is perpendicular to the plane.

High resistance measurement

The PPMS's capacity for measuring resistance in a four-point fashion is limited to mega ohms. In order to delineate the resistance change in the AFM state at low temperatures, we adapted a DC-IV method by using Keithley 6221 and 6430 for measuring high resistance. The current and voltage chosen in the resistance measurements are listed in Table S1.

Table S1. The setting details for Keithley 6221 and 6430 when recording high resistance data.

Circumstances in which high resistance exists	Temperature or field range	The Current sourced by 6221	The Voltage range chosen for 6430
RT in 0 T	2–8 K	10 nA	200 V
RT in 0.5 T	2–4 K	50 nA	20 V
MR at 2 K	0–0.6 T	10 nA	200 V
	0.6–0.8 T	10 nA	20 V
MR at 3 K	0–0.6 T	10 nA	200 V
MR at 4 K	0–0.5 T	10 nA	200 V
MR at 5 K	0–0.4 T	10 nA	200 V
MR at 6 K	0–0.3 T	10 nA	200 V
MR at 7 K	0–0.2 T	10 nA	200 V

Magnetoresistance for α and β-EuP_3

Figure S3 shows the resistivity with respect to the applied field at different temperatures for α and β-EuP_3 in left and right panel, respectively. α-EuP_3 shows a negative MR as long as the spin is polarized below 50 K. This negative MR likely comes from the anisotropic magnetoresistance which exists in ferromagnetic metal in general. As comparison, the resistivity for β-EuP_3 shows a colossal change in magnetic field at base temperature. Obviously the profile and magnitude of the MR are very different between the α and β-phases.

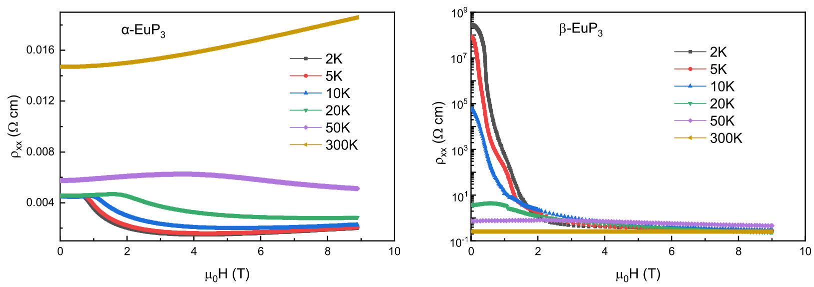

Fig. S3. Resistivity with respect to the applied field for α and β-EuP$_3$ when the field is perpendicular to the plane.

Hysteresis measurement

As shown is Fig. S4, the MR in β-EuP$_3$ shows no apparent hysteresis when the magnetic field is parallel along the stacking direction. This feature is essentially different from the large hysteresis in manganites due to the spatial separation in the first order MIT transition [2].

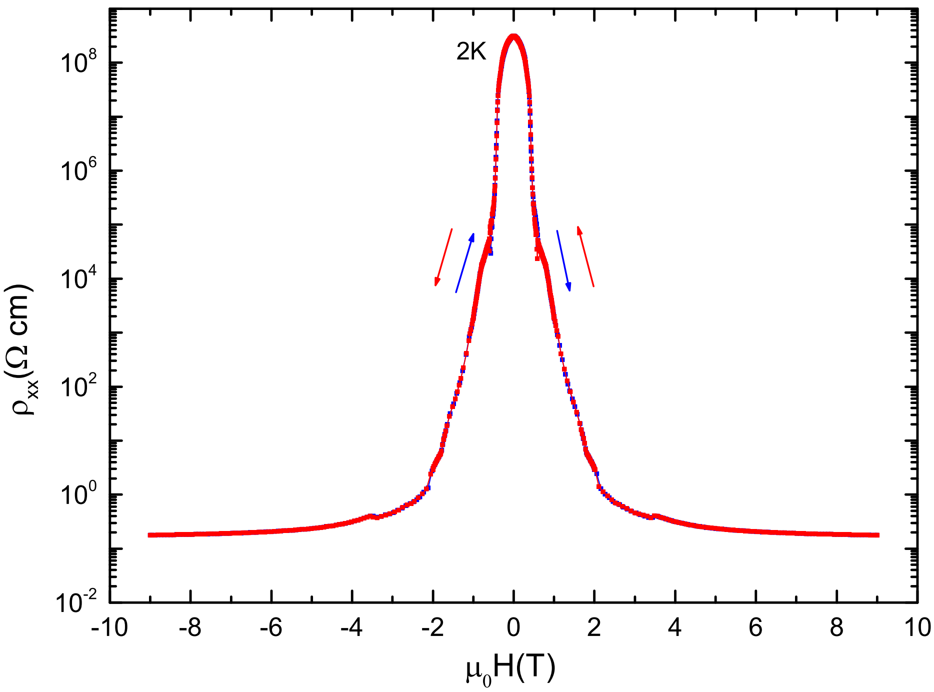

Fig. S4. The resistivity change in β-EuP$_3$ in a close loop from -9 T to +9 T to -9 T at 2 K.

Fitting of the $\rho_{xx}(T)$ in different magnetic field

In order to address the gap closing for β-EuP$_3$ in a magnetic field, we fit the $\rho(T)$ curves from 100 K to 300 K with an activated form ($\rho = \rho_0 e^{E_g/2k_BT}$). Figure S5 shows that the $\rho(T)$ curves in different magnetic fields approximately follow the activated form and the yielded band gap E_g is shown in Fig. 3 (d) in the main text.

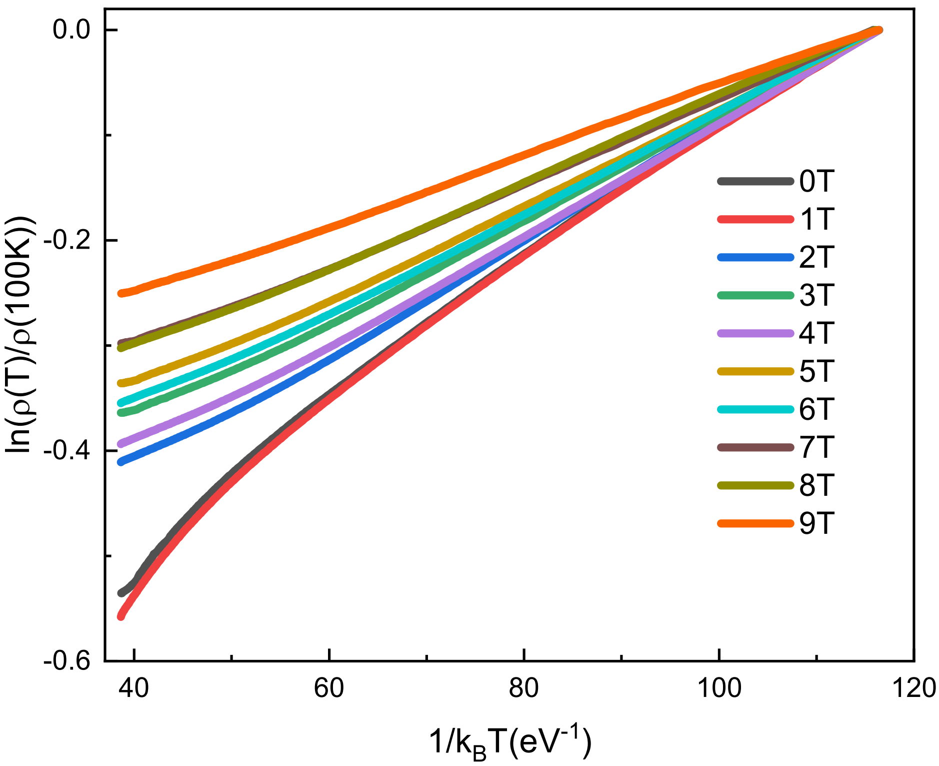

Fig. S5. The resistivity change in β-EuP_3 in a close loop from -9 T to $+9$ T to -9 T at 2 K.

Longitudinal MR when the direction of the external field is in the stacking plane

Figure S6 shows the magnetization and electrical properties of β-EuP_3 when the magnetic field is in the stacking plane. Because the moments align along in the stacking plane in the sequence of two-in-two-out, the magnetic field parrallel to this direction tends to induce a spin-flop transition. Figure S6 b shows the spin-flop transition occurs at 1 T and then a continuous rotation of the magnetic moment occurs upon increasing H, leading to a saturated magnetization at 2 T at based temperature. Such spin-flop trastion induces a steep change of resistivity in three orders of magnetude (Fig. S6 d). This feature is absent in the transversal MR when the magnetic field is parallel along the hard axis. Figure S6 e and f show that the $\rho(T)$ curves also manifest a hump-like feature which distincts a high-temperature semi-conductive and low-temperature metallic phases in the external fields higher than 2 T. When $\mu_0 H \leq 2.2\ T$, the $\rho(T)$ curves show a reentry to the insulator state a low temperature. The magnetization and resistivity measurements reveal that the reentry point overlap with the AFM transition points. There is no phase separation region apparently in the vicinity of the phase boundary (Fig. S7).

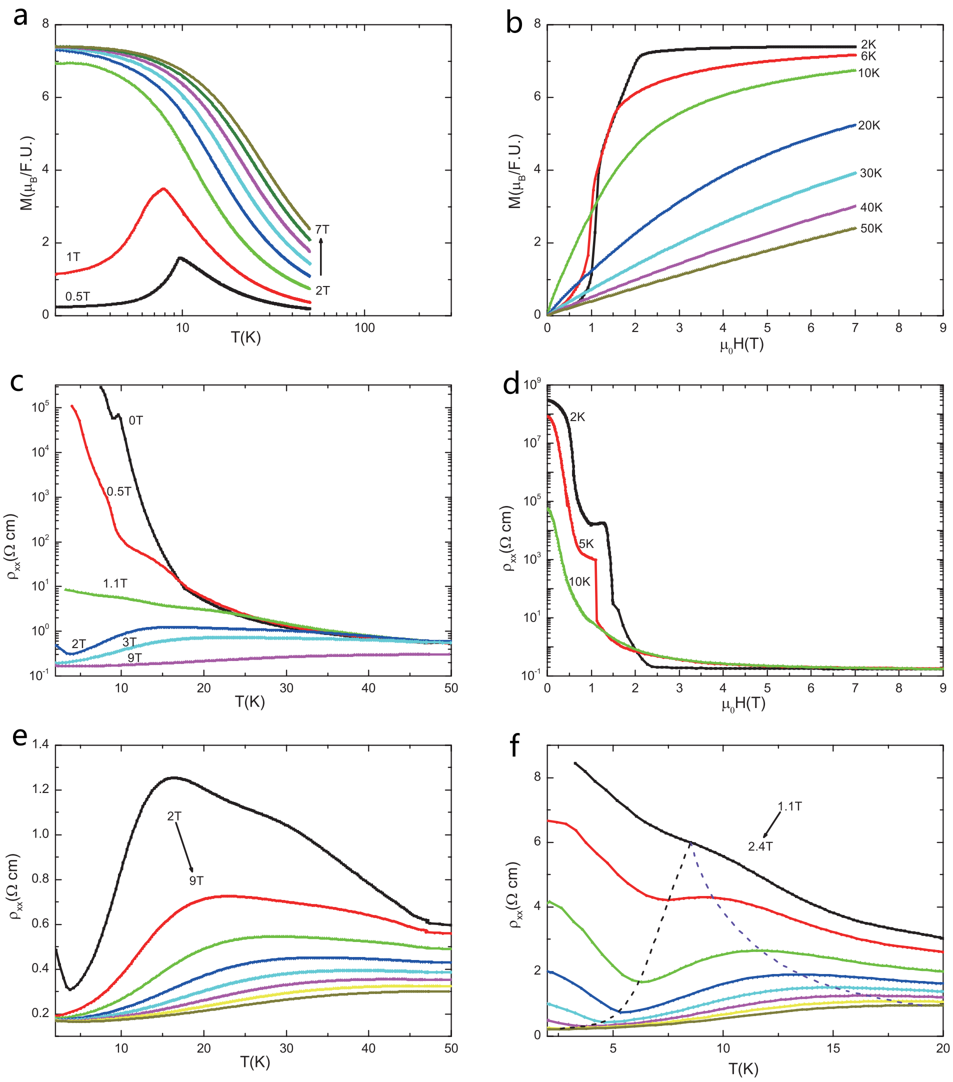

Fig. S6. Magnetic and electrical properties of β-EuP_3 when H is in the stacking plane. (a): magnetization (M) under different external magnetic fields ($\mu_0 H$) versus temperature. (b): M versus $\mu_0 H$ at different temperatures. (c): ρ_{xx} under several representative H versus temperature. (d): ρ_{xx} versus H at different temperatures. (e): Zoom-in of the panel (c) demonstrates a broad peak on the $\rho(T)$ curves for $\mu_0 H \geq 2$T. (f): Zoom-in of the panel (c) for 2 K $\leq T \leq$ 20 K demonstrates detailed features on the $\rho(T)$ curves including an MIT and an reentry of the insulating state overlapped with T_N when 2.2 T $\geq \mu_0 H \geq$ 1.1 T.

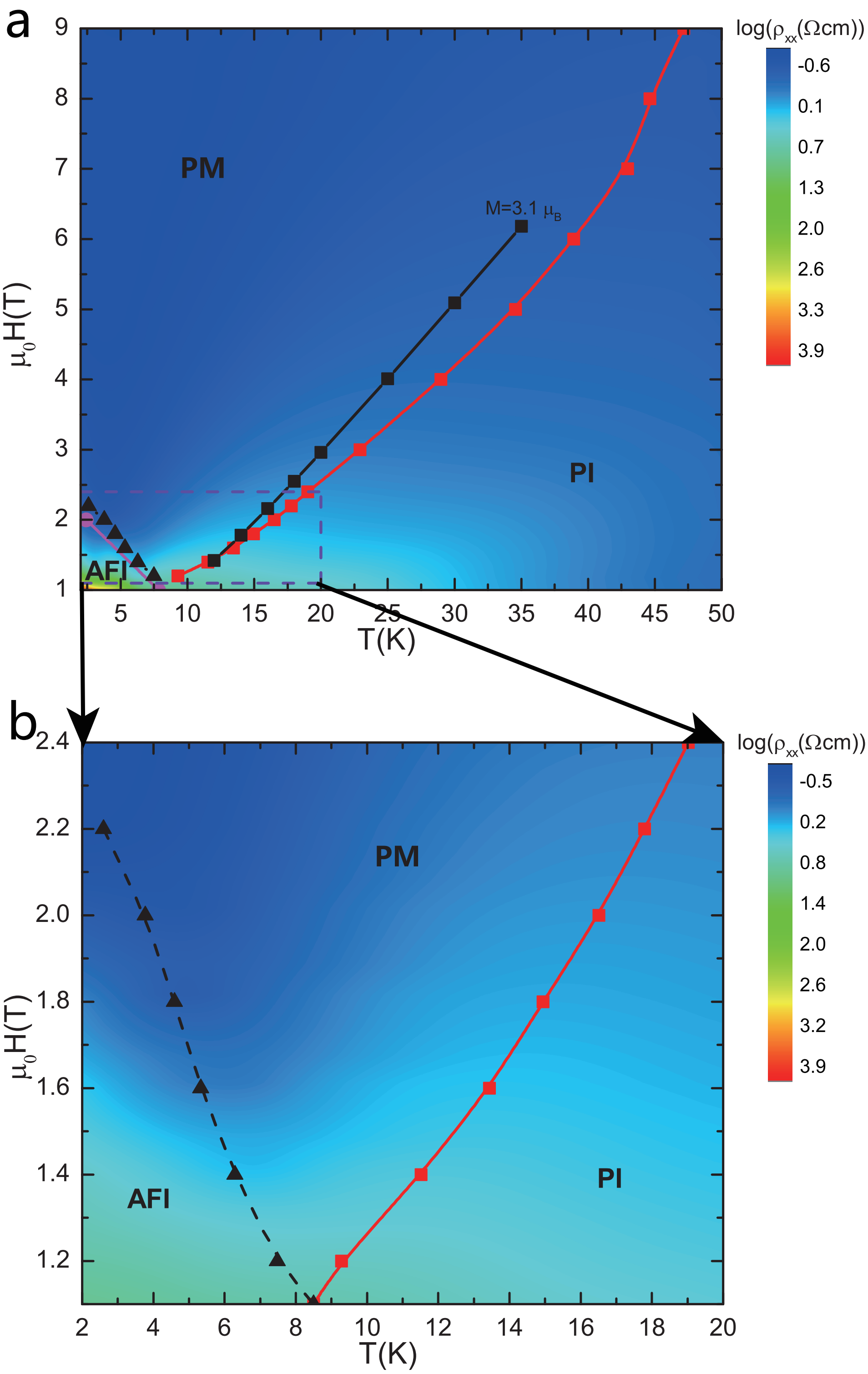

Fig. S7. Contour map in the H–T plane of for resistivity in β-EuP_3 when the field is in the stacking plane. The color bar at the side of the map represent the magnitude of the resistivity. The dots, squares and triangles denote the transition temperatures. PM, PI and AFI stand for the paramagnetic metal, paramagnetic insulator, and AFM insulator phase, respectively.(a): a full diagram for $\mu_0 H < 9\ T$ and $T < 50\ K$. The magenta dashed line, determined by magnetization, is the boundary between AFI and PM/PI ; the red dashed line is the boundary between PI and PM. The black dashed line, determined by resistivity, is the boundary between AFI and PM. The black dashed line is overlapped the magenta. (b) Zoom-in of the phase diagram for $1.1\ T < \mu_0 H < 2.4\ T$ and $2\ K < T < 20\ K$ show no phase separation of AFM and insulator states.

Resistance for another piece of β-EuP$_3$

We have measured several pieces of samples. All the samples in the experiment, which were obtained from the crystal growth described in the draft, behave similar in the $R(T)$ and $R(H)$ dependence. Figure S8 shows another piece of β-EuP$_3$ which has CMR at 10 K as well. Because its resistance is beyond the measurement upper limit of PPMS, we did not measure the MR below 10 K. Yet the profile of $R(T)$ and $R(H)$ is same as that for the piece of the sample shown in the text.

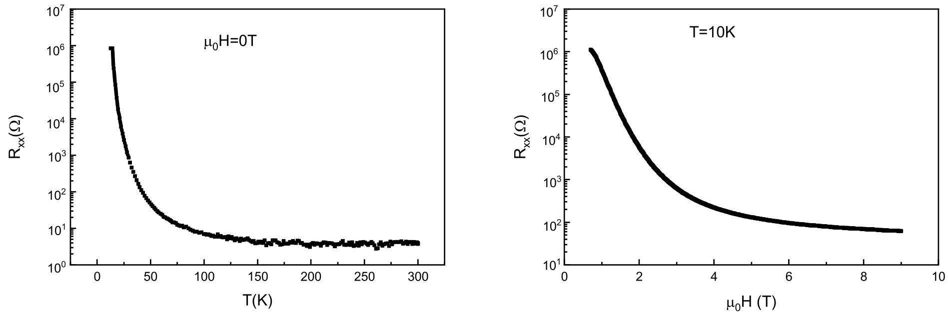

Fig. S8. Left panel: $R(T)$ curve for another piece of β-EuP$_3$. Right panel: Resistance versus magnetic field at 10 K.

---

* Electronic address: `gwljiashuang@pku.edu.cn`

[1] T Chattopadhyay, PJ Brown, P Thalmeier, W Bauhofer, and HG von Schnering. Neutron-diffraction study of the magnetic ordering in euas 3, eu (as 1- x p x) 3, and β-eup 3. *Physical Review B*, 37(1):269, 1988.

[2] Y Tokura and N Nagaosa. Orbital physics in transition-metal oxides. *science*, 288(5465):462–468, 2000.